Jurnal Tribologi 30 (2021) 133-148

MYTRIBOS Malaysian Tribology Society

Jurnal Tribologi

Website : jurnaltribologi.mytribos.org e-issn: 2289-7232

Optimum design of brake friction composites

Fikrat Yusubov *

Department of Mechanics, Azerbaijan State Oil and Industry University, 16/21 Azadliq Ave, Baku, AZERBAIJAN.
*Corresponding author: fikratyusub@gmail.com

KEYWORDS

Composites
Friction coefficient
Taguchi
Density
Hardness

ABSTRACT

The present study is aimed at developing a new friction material for medium or heavily loaded braking systems. The manufacturing parameters of low-metallic polymer-matrix brake friction composites were optimized using the plan of experiments based on the Taguchi method. The hot-pressing pressure, the duration of heating in the furnace and proportion of plasticizer are used as control parameters to design composites by conventional Powder Metallurgy Techniques. The physical-mechanical properties of produced materials characterized by properties like density and hardness. Standard L27 orthogonal array was chosen to conduct experiments and variable parameters were examined using the analysis of variance (ANOVA) technique. Signal-to-noise ratio (S/N) estimated by "larger-the-better" criterion for both output parameters. Prediction and modeling were performed on Minitab 19.1.1 software. Friction tests were conducted on pin-on-disc type friction and wear test machine model MMW-1. The obtained regression models were in good agreement with the statistically analyzed data. It was observed that pressure is the most significant factor affecting the physical-mechanical and friction characteristics of investigated composite materials.

1.0 INTRODUCTION

The friction materials are one of the most important parts of braking applications and clutch devices (Natarajan et al., 2012). The effectiveness of brake systems directly depends on the quality of the brake pad materials (Verma et al., 2016). Brake pad materials for the brake system should be designed to maintain stable tribological properties. Therefore, friction materials must

Received 5 June 2021; received in revised form 10 July 2021; accepted 14 August 2021.
To cite this article: Yusubov (2021). Optimum design of brake friction composites. Jurnal Tribologi 30, pp.133-148.

possess excellent physical-mechanical characteristics to provide reliable operations. Thermally stable and high mechanical properties materials could be a considerable choice in the composition of brake pads. The brake friction composites basically consist of the matrix or binder (mainly phenolic resin), fillers and reinforcing materials. Along with different organic or polymeric materials, friction composites typically contain metallic ingredients to improve their wear resistance, thermal properties and strength (Ficici et al., 2013). In addition to these components, almost all brake pads made in previous years contained asbestos. Nowadays in the field of tribology, one of the main trends is developing new eco-friendly, non-asbestos composite materials (Jadhav and Sawant, 2019). After banning asbestos due to health and environmental concerns in many countries around the world, researchers started to find alternatives. The role of polymer-based, organic materials has increased even more as asbestos friction materials have been removed from manufacturing, gradually. Polymer matrix composites are playing a significant role in the tribology industry because of their simple processing properties and cost-effectiveness (Sudeepan et al., 2014). The wide range of possibilities to change the structure of friction materials with different fibers or metal components using nanoparticles in polymer-based materials allows modifying tribological properties (Coetzee et al., 2020). These components can be used to improve certain characteristic features and performance of brake composites by changing their proportions. From this point of view, polymer-based composites reinforced with different fibers or metallic elements could be a good solution to replace asbestos.

In order to have a high and stable coefficient of friction at different sliding speeds and pressure conditions, the friction layer formed between the contact surfaces must have improved properties that can provide high tribological performance without damaging the base material at high temperatures. The formation of cracks, wear and decomposition processes on friction surfaces depend on physical parameters such as hardness, density and porosity (Crăciun and Pinca, 2016). Therefore, the brake pad and friction layer must have the required hardness and properties. In addition to the material factor, manufacturing parameters can also play a decisive role in achieving the desired properties (Aznifa et al., 2012; Modi et al., 2019). The satisfactory physical characteristics depend on the technological regimes and manufacturing parameters of the materials (Patil and Shirsat, 2020). This may include technological parameters such as mixing the components, compaction of powder materials in press die and heating conditions in the furnace.

However, conducting multiple experiments is not economically suitable. The design of experiments is one of the most powerful statistical methodologies to study the effect of different design parameters simultaneously. Comparing to the traditional methods, the Taguchi approach reduces drastically the number of experiments and offers useful distinctive elements like the Signal-to-Noise (S/N) ratio which is helping improve the quality of conducted work (Ranjit, 2010).

Numerous experimental works have been made to study the material selection and formulation effect of brake pads on tribological properties (Nilov et al, 2015; Österle and Urban, 2004). However, there are not many literature studies dedicated to the optimization of design parameters like hot-pressing pressure, duration time of heating in the furnace and volume fraction of plasticizer. Especially, the studies of the effect of plasticizers in the preparation of friction materials are very rare.

The brake friction material used in this work was prepared based on the non-asbestos organic type of formulation. The main objective of the present study is to determine optimum design parameters for preparing new composite materials based on Powder Metallurgy Techniques. For this purpose, low metallic phenolic resin brake friction samples were prepared on the basis of the selected planning matrix to understand the effects of control factors on performance properties.

2.0 MATERIALS AND METHODS

Eleven ingredients were selected as raw materials to prepare composite materials. The composite formulation was used by following weight proportions: 25% barite, 25% phenolic resin, 7% aluminum dioxide, 10% lead, 10% tin, 7% copper-graphite (80% Cu 20% C), 5% silicon dioxide and 5% wollastonite. Along with that 1 wt. % of molybdenum disulfide, magnesium oxide and brass chips also were used in composition for improving physical-mechanical properties and compaction process. The specimens were fabricated in rectangular form (in size of 22.9 × 15.7 × 7.8 mm) by Powder Metallurgy Techniques including ball milling, dry mixing (for 16 hours with a speed of 60 cycles/min on a horizontal drum mixer) and pre-forming at 10 MPa as shown in Figure 1. Hot pressing was conducted under 160°C. Specimens were molded in a steel die. During the compacting process, the pressure was released several times, because, in the process of polycondensation of phenol and formaldehyde, water vapor and other gases can leave the inner zones (Sugozu et al, 2016). The glycerin used as a plasticizer for improving powder processing. The manufacturing process is finished with the post-curing procedure in a muffle furnace for 5 hours in 140°C.

Figure 1: Specimen used in the experimental works (a) compact form (b) sintered form.

3.0 DESIGN OF EXPERIMENTS

The experiments were conducted as per the Taguchi (Taguchi and Konishi, 1987) L27 orthogonal array. Data processing was done using Minitab 19.1.1 statistical software. In the process of preparing the samples, it was determined that the following factors may affect the physical properties of the materials: pre-forming and hot-pressing pressures, the duration of heating in the furnace, the duration die-pressing, the temperature and duration of sintering of compacted samples and proportion of plasticizer. Due to many factors, simplifications were made and only focused on those factors whose effects were difficult to study. The heating of the samples in the mold and sintering temperature was regulated by the melting temperature of the components. Compared to pre-forming, in the hot pressing stage, the formation process occurs in a more complex form. Because of this, hot pressing was chosen as an important parameter. Thus, hot-pressing pressure (pressure), duration of heating in the furnace (time) and proportion of

plasticizer (plasticizer) used as control parameters to determine best quality characteristics (Table 1).

Table 1: Input parameters with different levels.

Control factors	Code	Unit	Level I	Level II	Level III
Pressure	A	MPa	10	17.75	25.5
Time	B	min.	10	35	50
Plasticizer	C	Wt.%	5	10	15

Signal-to-noise ratio (S/N) ratios were calculated using Equation (1) according to the "larger-the-better" criterion (Ross, 1988) for both output parameters:

$$\frac{S}{N} = -10 \log \left[\frac{1}{n} \sum_{i=1}^{n} \frac{1}{y_i^2} \right] \quad (1)$$

where y is the observed data for the given parameter level, n is the number of experiments. Each factor level combination was repeated three times and obtained average test results were used for data evaluation.

4.0 MEASUREMENT OF PHYSICAL-MECHANICAL PROPERTIES

The Archimedes method was applied to measure the density of samples using ISO 2738 standard. The hardness was measured using the Brinell hardness testing method with a load of 62.5 kg·f and a steel ball with a diameter of 2.5 mm (GOST 9012-59). The surface of the samples was grounded on a grinding machine with SiC papers (100, 1000 and 2000-grid) before each hardness test.

5.0 FRICTION TESTS

The dry sliding friction tests were performed on universal friction testing machine MMW-1 at room temperature. The rotating specimens were pressurized against a stationary steel disc (EN-32 steel hardened to 44-46HRC) as in the diagram presented in Figure 2. The outer diameter of the disc is 31.7 mm and the inner one is 13.0 mm. Cylindrical samples were used in the tests in size of Ø 4.7 × 12.8 mm. Friction tests were carried out at 7.69 MPa nominal contact pressure, 1.74 m/s sliding velocities and 1.57 km sliding distance (sliding time is 1400 sec).

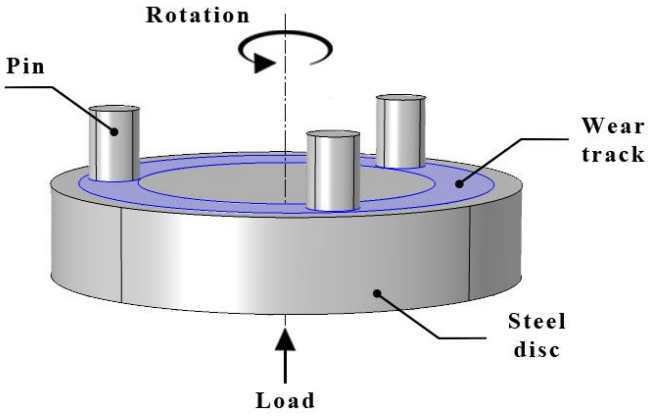

Figure 2: Schematic of pin-on-disc configuration.

6.0 RESULTS AND DISCUSSION

6.1 Physical and Mechanical Properties

The design matrix and test results are given in Table 2. As the per orthogonal array for each row, the obtained test results for density and hardness are transformed in S/N ratio. The tribological behavior of friction composites is determined by the characterization of the contact surfaces of the disc and brake pad (Eriksson and Jacobson, 2000). In this regard, it is important to analyze the surface structure of the brake pad materials.

The SEM images of the specimen are represented in Figure 3. Brake friction composites usually have rough surfaces. For this reason, the samples were polished with SiC paper to improve surface reflection.

Small scratches on the surfaces are caused by polishing. From the presented illustrations, it is seen that the surface structure of both materials is similar. Uneven distribution of the wear process on the surface results in the non-stability of the coefficient of friction. The formation of wear debris, contact plateaus and friction layers much depends on the wear mechanisms (Surojo et al., 2019). Therefore, it is important that the components are evenly distributed along the brake pad surface. From Figure 3 it can be observed that the particles are uniformly distributed along the surface and components were combined to good bonding with each other. However, the surface of the №24 sample is relatively dark. This is due to the high content of glycerin. Thus, this difference was manifested in all samples with a plasticizer content of 15%.

At high temperatures, the surface of the counter-body material begins to soften, and the empty cells begin to fill not only with organic elements but also with worn particles of metal elements. Thus, the process of undesirable oxidation and sintering on the surface is restored. This process hardens the surface layer of the brake pad, and as a result, the surface of the disc begins to scratch, in which case the abrasive particles play a decisive role. Also, welding (adhesion) may occur on the surface of the pad material with the softened disc (Kragelski, 1962). However, the presence of metal elements in the brake pad composite ensures an even distribution of pressure on the surface and a relative reduction in surface temperature due to heat transfer. Therefore, it is important that the degradation temperature of organic components such as phenolic resin is higher than the melting temperature of metallic elements. In other words, the plasticity and

quality of the friction layer or so-called “third body” with a heterogeneous structure have a significant effect on the friction and wear characteristics of the materials (Filip et al, 2002). The suitability of the mechanical properties of the friction layer to the counter-body is one of the main factors for wear resistance and friction stability. In this regard, metal particles such as tin and lead with low melting points were used in the composites.

Table 2: Results of experiments based on L27 (3^3) orthogonal array.

№	Pressure [MPa]	Time [min]	Plasticizer [wt.%]	Density [g/cm³]	S/N ratio [dB]	Hardness [HB]	S/N ratio [dB]	Friction coefficient [μ]	S/N ratio [dB]
1.	10.00	10	5	1.985	5.95521	36.7	31.2933	0.365	-8.75414
2.	10.00	10	10	2.102	6.45265	37.0	31.3640	0.377	-8.47317
3.	10.00	10	15	1.992	5.98579	36.8	31.3170	0.362	-8.82583
4.	10.00	35	5	2.108	6.47741	38.5	31.7092	0.384	-8.31338
5.	10.00	35	10	2.128	6.55943	38.9	31.7990	0.383	-8.33602
6.	10.00	35	15	2.107	6.47329	38.6	31.7317	0.388	-8.22337
7.	10.00	50	5	1.983	5.94645	36.5	31.2459	0.366	-8.73038
8.	10.00	50	10	2.134	6.58389	37.3	31.4342	0.378	-8.45016
9.	10.00	50	15	1.991	5.98143	36.1	31.1501	0.362	-8.82583
10.	17.75	10	5	2.178	6.76116	39.4	31.9099	0.389	-8.20101
11.	17.75	10	10	2.221	6.93097	40.2	32.0845	0.405	-7.85090
12.	17.75	10	15	2.181	6.77311	39.7	31.9758	0.394	-8.09008
13.	17.75	35	5	2.189	6.80492	40.5	32.1491	0.413	-7.68100
14.	17.75	35	10	2.193	6.82077	41.0	32.2557	0.419	-7.55572
15.	17.75	35	15	2.188	6.80095	40.7	32.1919	0.408	-7.78680
16.	17.75	50	5	2.179	6.76514	39.2	31.8657	0.389	-8.20101
17.	17.75	50	10	2.186	6.79300	40.4	32.1276	0.401	-7.93711
18.	17.75	50	15	2.176	6.75318	40.0	32.0412	0.397	-8.02419
19.	25.50	10	5	2.292	7.20429	42.6	32.5882	0.422	-7.49375
20.	25.50	10	10	2.326	7.33219	43.3	32.7298	0.439	-7.15071
21.	25.50	10	15	2.290	7.19671	43.1	32.6895	0.430	-7.33063
22.	25.50	35	5	2.338	7.37689	43.7	32.8096	0.438	-7.17052
23.	25.50	35	10	2.340	7.38432	44.2	32.9084	0.444	-7.05234
24.	25.50	35	15	2.336	7.36946	43.8	32.8295	0.433	-7.27024
25.	25.50	50	5	2.289	7.19292	41.9	32.4443	0.410	-7.74432
26.	25.50	50	10	2.295	7.21565	42.8	32.6289	0.422	-7.49375
27.	25.50	50	15	2.288	7.18912	42.6	32.5882	0.423	-7.47319

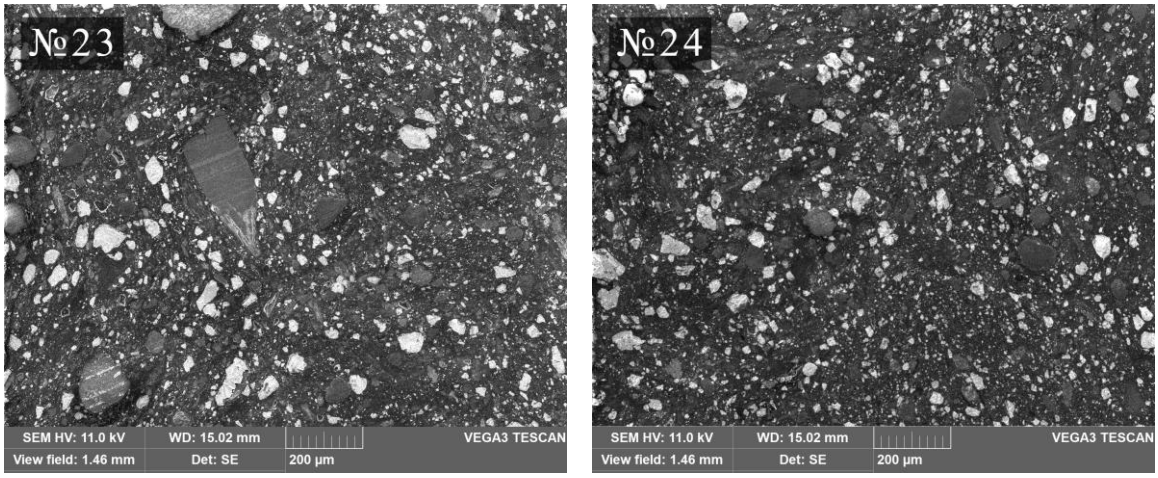

Figure 3: The SEM images of samples prepared for experiments №23 and 24.

The rankings of design parameters for mean S/N ratios of density and hardness are given in Table 3.

Table 3**:** Response table for S/N ratios for (a) density and (b) hardness.

Level	Pressure	Time	Plasticizer
1	6.268	6.732	6.720
2	6.800	6.896	6.897
3	7.274	6.713	6.725
Delta	1.005	0.183	0.176
Rank	1	2	3

(a)

Level	Pressure	Time	Plasticizer
1	31.45	31.99	32.00
2	32.07	32.26	32.15
3	32.69	31.95	32.06
Delta	1.24	0.32	0.15
Rank	1	2	3

(b)

In respect of S/N ratio calculation, the most important factors which are influencing the process have been determined (as shown in Figure 4). It was found that pressure is the most important factor affecting both properties. The obtained plots reflect the given average S/N values in Tables 3 and show the most important factors influencing the process.

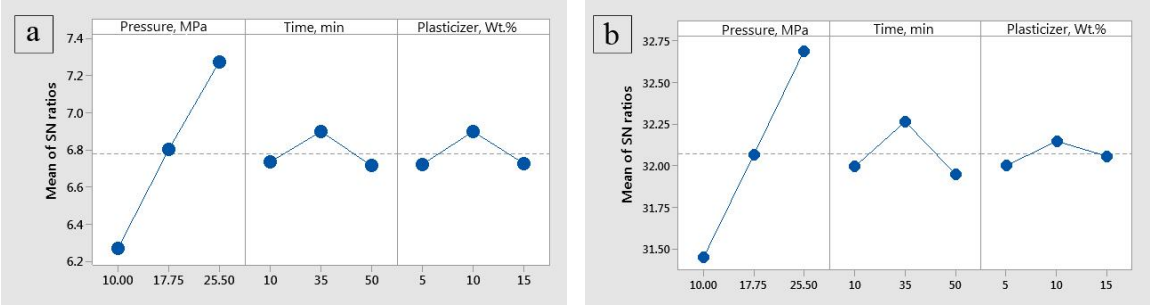

Figure 4: Main effect plot (data means) for the (a) density and (b) hardness.

Processing of obtained test results by ANOVA helped to analyze the factors and interactions influencing the density and hardness (Table 4 and 5).

Table 4: ANOVA table for density

Source	DF	Seq SS	Adj SS	Adj MS	F-value	P-value	P, %
A	1	0.284761	0,374926	0.006120	0.006120	0.030	86.79
B	1	0.000017	0,011732	0.010773	0.010773	0.006	0.01
C	1	0.000004	0,017749	0.010533	0.010533	0.006	
A*A	1	0.000062	0,000219	0.000062	0.000062	0.815	0.02
B*B	1	0.010966	0,001085	0.010966	0.010966	0.005	3.34
C*C	1	0.010696	0,019687	0.010696	0.010696	0.006	3.26
A*B	1	0.000603	0,000167	0.000603	0.000603	0.469	0.18
Error	19	0.021000	0,000333	0.021000	0.001105	0.030	6.40
Total	26	0.328109	0,012360	0.006120	0.006120	0.006	100.00

Table 5: ANOVA table for hardness

Source	DF	Seq SS	Adj SS	Adj MS	F-value	P-value	P, %
A	1	147,920	161,353	23,0505	208,90		90,50
B	1	0,000	1,660	1,6601	15,04	0,001	
C	1	0,320	9,712	9,7118	88,02		0,20
A*A	1	0,090	1,962	1,9621	17,78		0,05
B*B	1	11,067	0,090	0,0896	0,81	0,379	6,77
C*C	1	1,779	11,067	11,0674	100,30	0,000	1,09
A*B	1	0,178	1,779	1,7785	16,12	0,001	0,11
Error	19	2,096	0,178	0,1776	1,61	0,220	1,28
Total	26	163,450	2,096	0,1103			100,00

Where DF is degrees of freedom, Seq SS is the sequential sum of squares, Adj SS is the adjusted sum of squares, P is the percentage of contribution. Results showed that pressure is the most dominant control factor for density with 86.79% and hardness with 90,50%. The other control factors effect was only 0.01% - 0.20% for both output parameters. The 3D interpretation of the dependence between density and time-plasticizer factors showed an increase in heating time and plasticizer wt. % are increasing density up to the second level of these factors (Figure 5a) And after this point, density starts to decrease. A similar effect has been observed for hardness (Figure 5b).

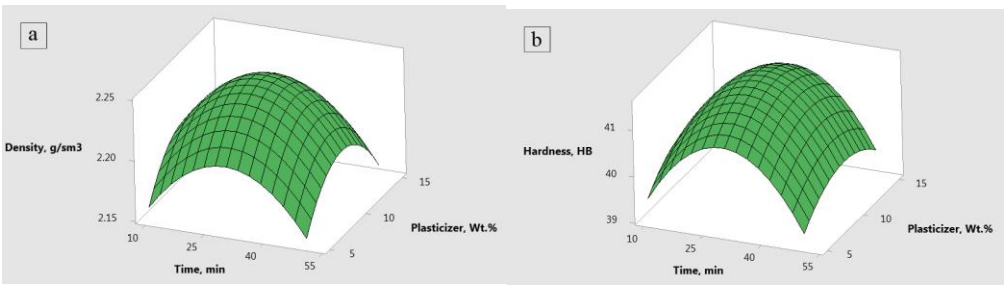

Figure 5: Surface plot for dependence between (a) density, (b) hardness and regime parameters.

The most important interaction factor for density was the combination of B*B (3.34%) and C*C (3.26%) and the most significant factor for hardness was a combination of B*B (6,77%).

The hardness of the obtained sample increases with an increase in the compaction pressure under mechanical influences. Consequently, compaction pressure has a major effect on the pore size of the composite materials. After high plastic deformation of powder particles lead to the formation of a denser microstructure. Furthermore, the increased particle contact area is resulting in a decrease in the porosity rate (Skrinjar and Larsson, 2004). The main purpose of pressing is to reduce the initial volume of powder by compression. However, during the deformation of the compact material, the volume remains constant and only the geometric dimensions change. During pressing, the volume of the powder product is decreasing due to the filling of the space between the particles as a result of mixing and plastic deformation. In this regard, one of the main factors affecting density is pressure. In the second stage, the already compressed particles begin to resist pressure, and during this time the density does not change. And finally, when the pressure exceeds the compressive resistance, the third stage-plastic deformation begins. As a result of plastic deformation, the particles become fixed to each other and the hardening process takes place (Michrafy et al., 2004). It is known that excessive pressure can cause defects in the structure of the compact material.

However, no matter how effective the compacting process, the micro-pores still remain inside the material. During post-curing, the process of volume reduction occurs again due to the reduction of porosity and thus the density of the composite increases. Post-curing is especially important for multi-component systems. Because multi-component systems have high free energy, post-curing is used to form concentration in the system.

It must also note that using glycerin as an inert plasticizer provides more effective contact between the particles and leads to uniform distribution density. The density distribution of compacting powder material is not nonhomogeneous due to interparticle friction and die wall friction (De Mello et al., 2001). Lubricants reduce friction between the particles themselves and friction of particles against the wall of the mold and have no effect on the properties of the compact material. As a surface-active lubricant, glycerin serves to distribute the pressure proportionally within the material by reducing friction on the outer and inner surface layer.

The results of the optimization are given in Table 6. It was determined that optimum levels are A (Level III), B (Level II) and C (Level II) for both output parameters.

Table 6: Optimum parameters.

Parameter	A	B	C	Output
Density	25.5	35	10	2.36804
Hardness	25.5	35	10	44.3296

The linear regression equation was applied to summarize the results of ANOVA, and the following models (2) and (3) were obtained for the density and hardness, respectively. For density and hardness, R^2 are 93.60% and 98.72%, and adjusted R^2 are 91.24% and 98.24%, respectively.

$$Density = 1.6479 + 0.01957A + 0.00759B + 0.0339C - 0.000054A^2 - 0.000115B^2 - 0.001689C^2 - 0.000034AB \quad (2)$$

(Unit of density is g/cm^3)

$$Hardness\ (HB) = 29.569 + 0.3223A + 0.2278B + 0.462C - 0.00203A^2 - 0.03659B^2 - 0.02178C^2 - 0.000777AB \quad (3)$$

Obtained regression models can be used to predict the quality of composites by means of physical-mechanical characteristics. Residual plots of linear regression model showing the distribution of the residual between the experimental results and the predicted values for the density and hardness also show that this model is adequate for the process (Figure 6). Residual values are calculated by the following equation (Teruo, 2011):

$$e = y - \hat{y} \quad (4)$$

where is the e is the residual, y is the experimental response value and $\hat{y}$ is the predicted response value.

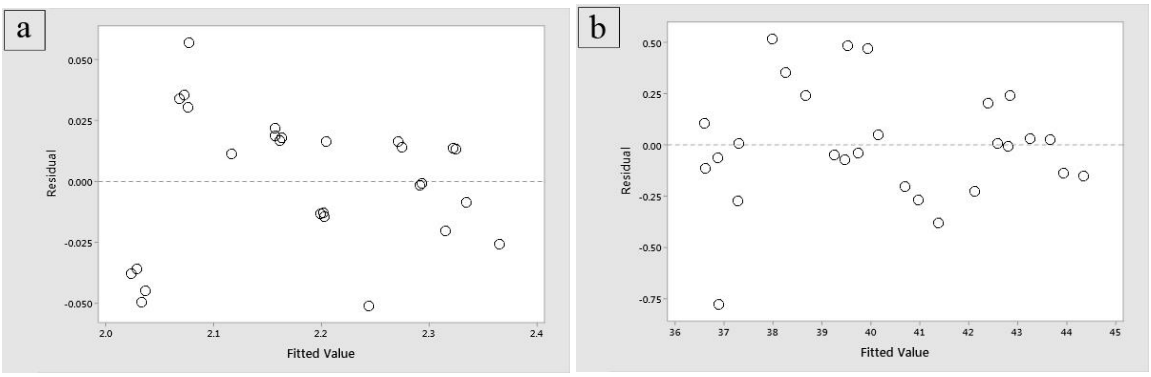

Figure 6: Residual plots of linear regression model for (a) density and (b) hardness.

6.2 Friction Performance

As seen in Table 2, the friction coefficient for the prepared composites varied in the range of 0.362-0.444. The highest friction coefficient was obtained with the sample having the highest hardness and density. In samples with low physical properties, the coefficient of friction was low. The results of ANOVA have shown that the most important factor in increasing the coefficient of friction is the pressure (83.84%). The impact of other factors was relatively low. It was found that the percentage contribution of plasticizer and time is 0.15 and 0.04%, respectively. Figure 7. demonstrates the Pareto chart for the main factors and their combinations. Reference line 2.09 indicates that the factors crossing this value are statistically significant at the 0.05 level for the given model. The most important of the interactions was the time*time (CC) combination with 9.86%.

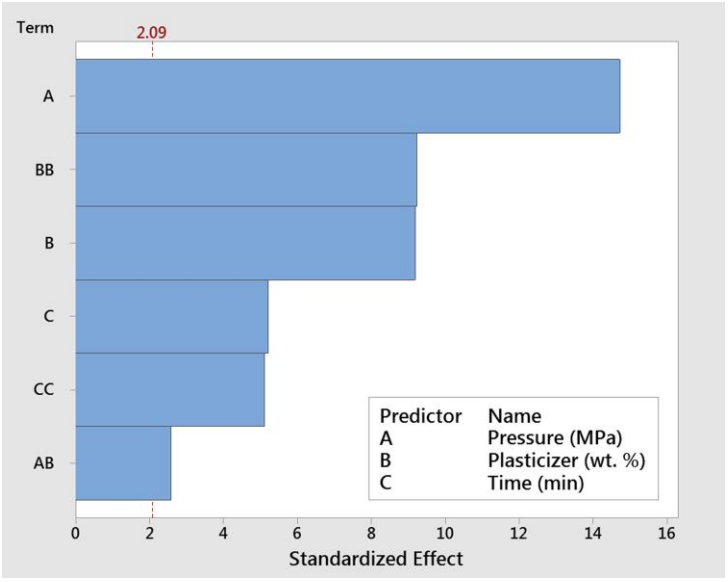

Figure 7: Pareto chart of the standardized effects for friction coefficient.

The effect of pressure on the coefficient of friction can be attributed to physical properties. As discussed above, pressure plays an important role in the integration of components. The addition of plasticizers further improves the forming process. These relations between factors were also confirmed by the regression equation (5) which can be forecast the friction coefficient (μ):

$$\mu = 0.26975 + 0.004212A + 0.002917C + 0.00748B - 0.000044C^2 - 0.000362B^2 - 0.000021AC \quad (5)$$

For the obtained model R^2 is 97.68 % and adjusted R^2 is 96.99%. When the physical properties are sufficiently stable, the tribological properties are also stable, which is reflected in the behavior of friction and wear. Figure 8 shows SEM images of the brake friction samples. The codes in the SEM images indicate the number of experiments performed according to the design matrix.

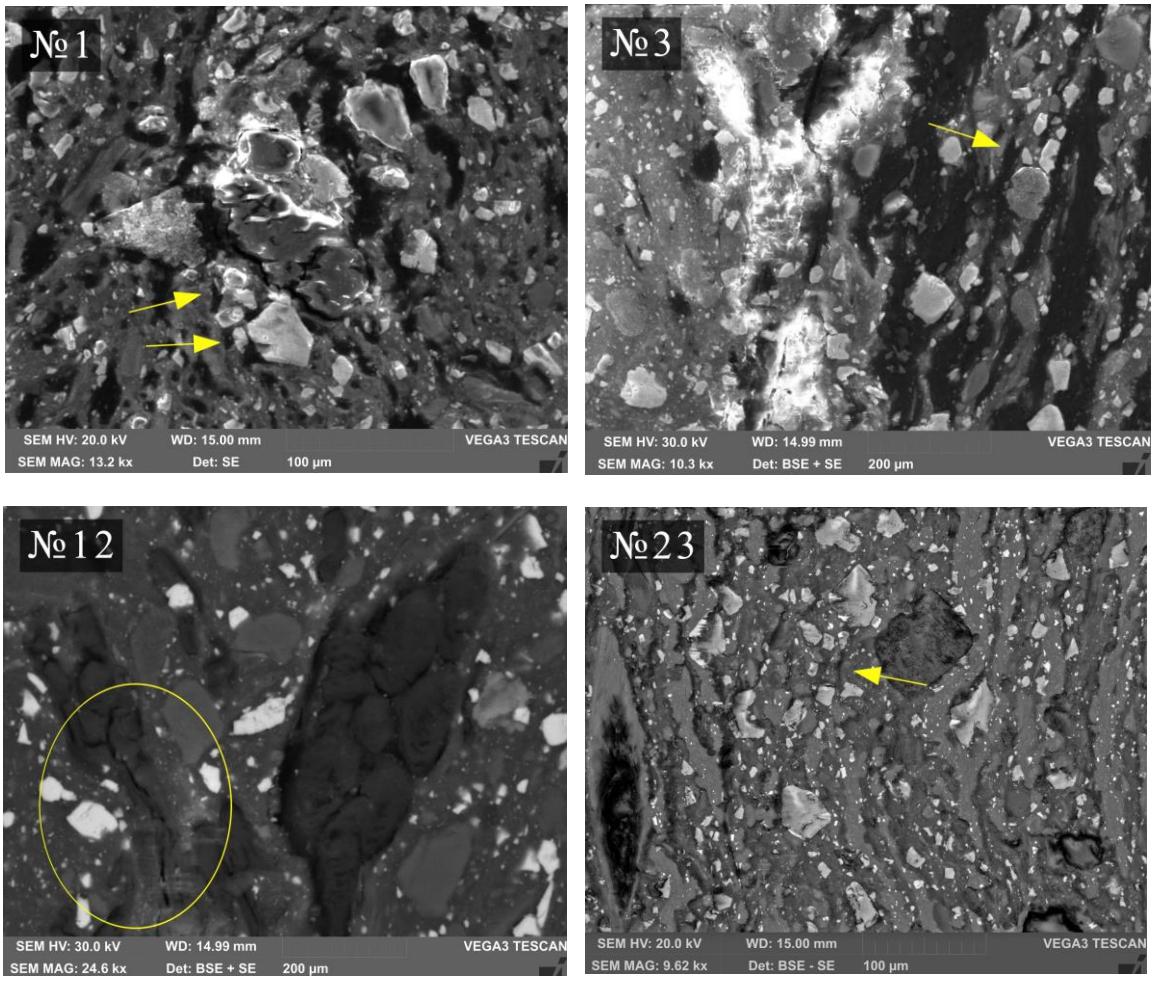

Figure 8: SEM micrographs of worn surfaces.

Specimens with low density and hardness were characterized by a relatively rougher surface. It is known that the tribological behavior of contacting couples depends on surface morphology (Aher et al., 2020). At the microscopic level, the contact of friction materials occurs in real contact areas under a given load. Because the friction surfaces are uneven, deformation and stress have different effects on different areas of the contact surface due to the viscoelastic properties of polymeric composites (Chang et al., 2018). As friction continues, the heat generated by the formation and destruction of friction bonds changes the surface morphology. Increased roughness in the morphology of the contact surface reduces the friction force. Therefore, the friction coefficient was low in samples with low physical properties. As can be seen from the SEM images, there is a large number of micro-voids and micro-cracks on the worn surfaces of samples №1 and 3, which have low physical properties. This can be explained by the fact that in these samples, due to the low hardness, the wear was also high. Micro-cracks observed on the contact surface of the samples indicate that plastic deformation has occurred in these materials. It is clear that during the degradation of organic components, the number of worn particles on the external

surface is also high, as the wear is high on low-hardness surfaces. An increase in temperature on the contact surface as a result of frictional heat release decomposes the organic components like phenolic resin, which in turn cannot sufficiently bind all the ingredients of the composite. Therefore, cracks form on the surface and wear particles increase (Nawangsari et al., 2019). Worn particles compressed on the steel surface participate in the friction process by forming a new friction layer in repeated dry sliding. This reduces wear over time and helps stabilize the coefficient of friction (Österle and Urban, 2004). In the process of friction, wear debris forms secondary plateaus as a result of compaction (Eriksson and Jacobson, 2000). As the contact area increases with the formation of the secondary plateaus, the coefficient of friction increases over a certain time period. However, the presence of solid abrasive particles such as Al_2O_3 or SiO_2 plays a special role in the wearing process. The presence of solid particles on the contact surface during friction intensifies the wear. Along with that, the movement of abrasive particles depends on the surface morphology and the hardness of friction surfaces (Manoharan et al., 2014). The reason why micro-voids are larger in these samples can also be attributed to metallic particles. During friction, detaching and falling metallic particles can intensify wear and increase micro-voids. All these wear mechanisms play an important role in changing the morphology of the surface layer. Friction tests have shown that abrasive wear is common in all samples prepared.

In addition, wear debris is found in almost all samples which were marked with yellow arrows in the SEM images. It is very important that the surface components are uniformly distributed, as the wear debris accumulates on the interface during friction and forms a friction layer. However, the simultaneous occurrence of several friction mechanisms in the sliding process, accompanied by various chemical reactions, affects the formation of a friction layer on the contact surface. Figure 8 (№12 and 23) illustrates that worn surfaces of composites with better physical properties were smoother contact surfaces than other prepared samples. Manoharan et al., (2018) studied the effect of different graphite forms on the tribological behavior of brake friction materials. It was found that under elevated temperatures in the phenolic resin-based brake friction composites plastic deformation occurs and thin graphite layer forms along the sliding direction at the friction surface. The formed graphite layer prevents plastic deformation by covering the worn surface and stabilizes the coefficient of friction by improving the smoothness of the surface. Similar effects were observed on the worn surface of almost all samples. Besides graphite and molybdenum disulfide, it is known that copper also acts as a solid lubricant at high temperatures as a result of recrystallization of nanocrystals (Kumar and Bijwe, 2011). Consequently, the presence of solid lubricants further contributed to the formation of smooth surfaces in relatively high-density samples like composites №12 and 23. The surface morphology of these composites shows no sign of complex wear mechanisms. A relatively small number of wear debris particles were observed in these samples, and no large contact plateau formation was found. As discussed above, one of the reasons for the formation of micro-cracks is the degradation of the phenolic resin binder (Rajan et al., 2018).

However, due to the improved integration between the components and the high density, micro-cracks were observed in relatively small amounts in these samples. The SEM image taken for sample №12 with 0.394 friction coefficient shows relatively large cracks and decomposition signs of the contact surface (marked with a yellow circle). This can be attributed to the following reasons. The hollow points, which are common to the surface microstructure of №12 and other samples, played an important role in the friction process. This is due to the fact that the solid particles that were removed off from the contact surfaces as a result of wear fall into these hollow points. Although this increases the wear resistance over time, excess frictional heat causes cracks

to grow on the surface in areas with hollow spots (Liew and Nirmal, 2013). However, due to the heterogeneous structure of the composite materials, these processes such as abrasion or formation of hollow spots and fiction layer may be different depending on the friction regimes and wear mechanisms.

The mean of density, hardness and friction coefficient of the prepared specimen showed similar characteristics to each other. The specimen having a high hardness or density exhibited high friction coefficient.

7.0 CONCLUSIONS

In the present work, low metallic polymer-based brake friction composites were developed by Powder Metallurgy Techniques with various manufacturing parameters. Using the Taguchi technique, the following conclusions can be made on the basis of statistical processing of the obtained experimental data:

(a) The ANOVA observation showed that pressure most dominant factor for density and hardness, respectively 86.79% and 90.50%.
(b) Optimal combination for density and hardness was determined to be 25.5 MPa pressure, 35 min. heating time and 10 wt. % plasticizer.
(c) Regression models also confirmed that pressure had positively related to the process.
(d) The model fits with 93.60% and 98.72% (for density and hardness, respectively), between the observed actual experimental values and the predicted values.
(e) The results showed that the higher the physical properties, the higher the coefficient of friction. In general, the coefficient of friction for all samples ranged from 0.362 to 0.444.

REFERENCES

Aher, V.S., Shirsat, U., Wakchaure, V.D., VenkateshM., A., Amrutvahini (2020). An experimental investigation on tribological performance of UHMWPE composite under textured dry sliding conditions. Jurnal Tribologi, 24, 110-125.

Aznifa, Z., Jaafar, T.R., Berhan, M.N., Budin, S., Aziurah, M.S. (2012). Taguchi method for optimizing the manufacturing parameters of friction materials. International Journal of Mechanical and Materials Engineering, 7, 83-88.

Chang, Y. H., Joo, B.S, Lee, S.M., Jang, H. (2018). Size effect of tire rubber particles on tribological properties of brake friction materials. Wear, 394–395, 80-86.

Coetzee, D. & Venkataraman, M., Militky, J., Petru, M. (2020). Influence of nanoparticles on thermal and electrical conductivity of composites. Polymers, 12(4), 742.

Crăciun, A. & Pinca, C. (2016). Advanced materials with natural fibred reinforced aluminum composite for automotive brake disc. Solid State Phenomena, 254, 91-96.

De Mello, J.D.B., Binder, R., Klein, A.N., Hutchings, I.M. (2001). Effect of compaction pressure and powder grade on microstructure and hardness of steam oxidised sintered iron. Powder Metallurgy, 44, 53-61.

Eriksson, M. & Jacobson, S. (2000). Tribological surfaces of organic brake pads. Tribology International, 33, 817–827.

Ficici, F., Durat, M., Kapsiz, M. (2013). Optimization of tribological parameters for a brake pad using taguchi design method. Journal of the Brazilian Society of Mechanical Sciences and Engineering, 36 (3), 653-659.

Filip, P., Weiss, Z. Rafaja, D. (2002). On friction layer formation in polymer matrix composite materials for brake applications. Wear, 252, 189-198.

Jadhav, S.P. & Sawant, S.H. (2019). A review paper: development of novel friction material for vehicle brake pad application to minimize environmental and health issues. Materials Today, 19 (2), 209-212.

Kragelski, I.V. (1962). Friction and Wear. Mashgiz, Moscow.

Kumar, M and Bijwe, J. (2011) Non-asbestos organic (NAO) friction composites: role of copper; its shape and amount. Wear, 270, 269-280.

Liew, K. W., & Nirmal, U. (2013). Frictional performance evaluation of newly designed brake pad materials. Materials & Design, 48, 25–33.

Manoharan, S., Suresha, B., Bharath, P.B., Ramadoss, G. (2014). Investigations on three-body abrasive wear behaviour of composite brake pad material. Plastic and Polymer Technology. 3 (1), 10-18.

Manoharan, S., Vijay, R., Lenin, S. D., Kchaou, M. (2018). Experimental Investigation on the tribo-thermal properties of brake friction materials containing various forms of graphite: a comparative study. Arabian Journal for Science and Engineering, 44 (2), 1459–1473.

Michrafy, A., Dodds, J.A., Kadiri, M.S. (2004). Wall friction in the compaction of pharmaceutical powders: measurement and effect on the density distribution. Powder Technology, 148 (1), 53-55.

Modi, M., Agarwal, G., Veerandra, P., Bhatia, U., Pancholi, R. (2019). Parametric optimization in drilling of Al-SiC composite using Taguchi method. International Journal of Scientific & Technology Research, 8 (9), 2019-2022.

Natarajan, M. P., Rajmohan, B., Devarajulu. S. (2012). Effect of ingredients on mechanical and tribological characteristics of different brake liner materials. International Journal of Mechanical Engineering and Robotics Research, 1 (2), 135-157.

Nawangsari, P., Jamasri, J., Rochardjo H. S. B. (2019). Effect of phenolic resin on density, porosity, hardness, thermal stability, and friction performance as a binder in non-asbestos organic brake pad. IOP Conf Series: Materials Science and Engineering, 547, 1-8.

Nilov, A.S., Kulik, V.I., Garshin, A.P. (2015). Analysis of friction materials and technologies developed to make brake shoes for heavily loaded brake systems with disks made of a ceramic composite. Refractories and Industrial Ceramics, 56 (4), 57-68.

Österle, W. & Urban, I. (2004). Friction layers and friction films on PMC brake pads. Wear, 257, 215–226.

Patil, V.K., Shirsat, U.M. (2020). Influence of compressing pressure and sintering temperature on microstructure and mechanical properties of Ni-Cr based composites. Jurnal Tribologi, 26, 1-15.

Rajan, B.S., Balaji, M.A.S., Sathickbasha, K., Hariharasakthisudan, P. (2018). Influence of binder on thermomechanical and tribological performance in brake pad. Tribology in Industry, 40 (4), 654-669.

Ranjit, K.R. (2010). A Primer on the Taguchi Method. Second Edition, Society of Manufacturing Engineers.

Ross, P. J. (1988). Taguchi techniques for quality engineering, Mcgraw-hill book company.

Skrinjar, O. & Larsson, P. L. (2004). Cold compaction of composite powders with size ratio. Acta Materialia, 52, 1871–1884.

Sudeepan, J., Kaushik, K, Barman, T.K., Prasanta, S. (2014). Study of friction and wear of Abs/Zno polymer composite using Taguchi Technique. Procedia Manufacturing, 6, 391–400.

Sugozu, I, İbrahim, M., Sugözü, B. (2016). The Effect of ulexite to the tribological properties of brake lining materials. Polymer Composites, 39, 1-8.

Surojo, E., Ariawan, D., Arsada, R., Muhayat, N., Raharjo, W.W., Smaradhana. D.F. (2019). Effect of nitrile butadiene rubber (NBR) on mechanical and tribological properties of composite friction brakes. Tribology in Industry, 41 (4), 516-525.

Taguchi, G. and Konishi, S. (1987) Taguchi Methods Orthogonal Arrays and Linear Graphs: Tools for Quality Engineering. American Supplier Institute, Dearborn, Michigan.

Teruo, M. (2011). Taguchi methods benefits, impacts, mathematics, statistics, and application. ASME Press.

Verma, P.C, Menapace, L., Bonfanti, A., Aswath, P., Straffelinia, G., Gialanella, S. (2016). Role of the friction layer in the high-temperature pin-on-disc study of a brake material. Wear, 346-347, 56-65.